

Marginally jammed states of hard disks in a one-dimensional channel

Yuxiao Zhang, M. J. Godfrey, and M. A. Moore

Department of Physics and Astronomy, University of Manchester, Manchester M13 9PL, United Kingdom

(Dated: October 23, 2020)

We have studied a class of marginally jammed states in a system of hard disks confined in a narrow channel—a quasi-one-dimensional system—whose exponents are not those predicted by theories valid in the infinite dimensional limit. The exponent γ which describes the distribution of small gaps takes the value 1 rather than the infinite dimensional value 0.41269 Our work shows that there exist jammed states not found within the tiling approach of Ashwin and Bowles. The most dense of these marginal states is an unusual state of matter that is *asymptotically* crystalline.

I. INTRODUCTION

There has been remarkable progress in our understanding of the properties of marginally [1, 2] jammed states of hard spheres [3–8]. The most striking predictions are for the values of the exponents that describe the geometry of the marginally jammed system of hard spheres, such as the distribution of small gaps h between the spheres, $g(h) \sim 1/h^\gamma$, as $h \rightarrow 0$. The exponent $\gamma = 0.41269 \dots$, according to the infinite-dimensional replica-symmetry-breaking [9] mean field theory [7]. Numerical results in dimensions $d = 3$ to 10 [4] are consistent with the exponent being independent of dimension and equal to its value for $d \rightarrow \infty$.

This is a striking result which remains unexplained. Indeed, possible issues with the infinite-dimensional approach applied to $d = 3$ have been noted in [10]. There is also evidence that the exponents might not actually be independent of dimension, at least for shear-driven (and hence anisotropic) jammed states [11]. Despite this, it is commonly expected that the “upper critical dimension” is 2 [4, 12–17]. That is, the exponents should maintain their infinite-dimension values down to two dimensions; this expectation is supported by numerical evidence for logarithmic corrections to scaling in $d = 2$ [18–20]. In this paper we present evidence that marginally-jammed states in a one-dimensional system of hard disks have very different values for the exponents; for example, we find that $\gamma = 1$ exactly. Our result therefore provides further evidence for an upper critical dimension for marginally-jammed packings. The arguments of Refs. [12, 13, 16, 17] are Imry-Ma style arguments for 2 as the upper critical dimension: they do not provide numerical values for (or even demonstrate the existence of) exponents such as γ if the system dimension is below 2. The present work does both.

The one-dimensional system of hard disks in a narrow channel has been extensively studied in other contexts [21–33]. The channel width available to the centers of the disks has in this paper the value $\tilde{h} = 0.95\sigma$ so that the disks, which have diameter σ , cannot pass each other, but can touch their nearest and next-nearest neighbors, as shown in Fig. 1. The packing fraction ϕ is defined as $\phi = N\pi\sigma^2/(4H_dL)$, where N is the number of disks in a channel of length L and width $H_d = \tilde{h} + \sigma$.

The jammed states for channel widths $\tilde{h} < \sqrt{3}\sigma/2$ have already been studied [26, 34]. The complexity of these jammed states (which is the logarithm of the total number of jammed

states divided by N) is non-zero and all of the states are isostatic, in that there are just enough contacts to ensure stability. However, when $\tilde{h} < \sqrt{3}\sigma/2$ there are no small gaps at all between the disks, whereas for the range of \tilde{h} studied in this paper, $\sqrt{3}\sigma/2 < \tilde{h} < \sigma$, there are gaps that can be arbitrarily small: their distribution is described by the exponent $\gamma = 1$. The jammed states with arbitrarily small gaps have non-zero complexity and are isostatic; however, there are also jammed states in this system that are not isostatic but hyperstatic, and these have a much higher complexity according to the results of Ashwin and Bowles [35].

Recently Ikeda [36] has studied disks in a narrow channel when the diameters of the disks have a dispersion in size and obtained $\gamma = 0$ for the gap exponent. Polydispersity like this is often used in numerical simulations of glasses to speed up the simulations [37], or to discourage crystallization. Polydispersity is unphysical for molecular glasses: molecules actually have the same size. For disks in a narrow channel crystallization does not occur, except at the highest possible density. A small amount of polydispersity will convert the hyperstatic jammed states of the type discussed by Ashwin and Bowles into isostatic states, just as happens for crystals [38, 39]. Ikeda’s work allows a study of whether its use is harmless by finding the value of γ for the isostatic states which it produces. Ikeda [40] has argued that above the upper critical dimension, exponents like γ should not depend on whether polydispersity has been used to produce the isostatic states. This claim is apparently at variance with the simulational study of Ref. [39] in $d = 3$, which is above the upper critical dimension. In $d = 1$ (below the upper critical dimension), our isostatic states have $\gamma = 1$, which is very different from the case of isostatic states obtained by adding polydispersity: these have $\gamma = 0$, according to Ref. [36].

Ashwin and Bowles [35] had in fact claimed to have constructed the complete jamming landscape for disks all of the same size when $\sqrt{3}\sigma/2 < \tilde{h} < \sigma$. They argued that all the jammed states in the system could be constructed from 32 varieties of tile together with rules limiting which tiles could be joined to other tiles. Figure 1 shows two configurations that can be described by their tiling procedure: a unit cell of the state of maximum density (the “buckled crystal”) and an asymmetric pentagon. In the tiling picture, the gaps between disks take on a finite number of nonzero discrete values. However, we have discovered that the Ashwin-Bowles picture is incomplete: there are jammed states that would require an *infi-*

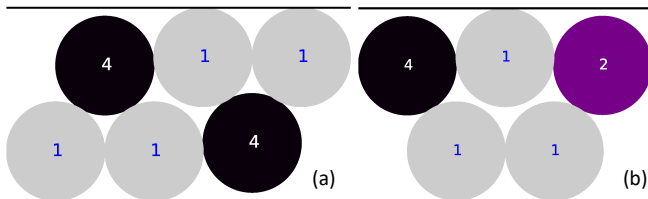


FIG. 1. (a) A unit cell of the buckled crystal, which is the jammed state of maximum density. Its packing fraction is $\phi \simeq 0.8074$. (b) An asymmetric pentagon, which is one of the Ashwin-Bowles tiles [35]. Labels 1, 2, 4 refer to particular values of y , as described in the text. The color coding is given in Fig. 3.

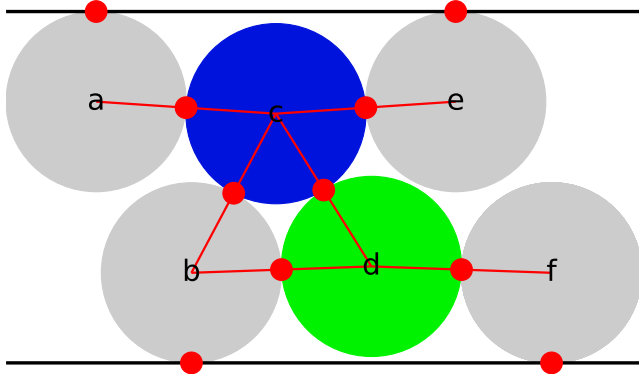


FIG. 2. Diagram to illustrate an algorithm for generating jammed states, as discussed in the text. Red dots denote contacts and red lines join the centers of disks that are in contact. The color coding follows Fig. 3.

nite number of tiles. We first became aware of this by studying the jammed states produced by Lubachevsky-Stillinger [41] quenches: these states regularly contained jammed disks at distances from the walls that were not among those considered by Ashwin and Bowles. In fact, some quenched states include short “sandwich states”; for example, in the jammed state shown in Fig. 3(g), the region to the left can be constructed from the Ashwin-Bowles tiles, while the right-hand portion consists of a short sandwich state. As a consequence of this, we shall not be using the tiling approach.

Our work is mainly analytical; we resort to numerical methods only to verify the stability of the jammed states. The numerical methods are described in the Appendix. In Sec. II we describe the algorithm used to generate the sandwich states. In Sec. III we show that these states are stable in some ranges of N . In Sec. IV we determine the value of the exponent γ in these jammed states and investigate the distribution of small contact forces to determine another commonly studied exponent, θ .

II. THE ALGORITHM

The coordinates of a disk will be labelled (x, y) , where y is measured from the mid-point of the channel. A disk which is just touching a wall has $y = \pm y_1$, where $y_1 = \tilde{h}/2$; it will

be referred to as a 1-disk (see Fig. 1). A 4-disk may have positions $\pm y_4$, where $y_4 = \sqrt{3}\sigma/2 - \tilde{h}/2 \simeq 0.391025$ (we set $\sigma = 1$ in this paper). It is at the apex of an equilateral triangle whose other vertices are 1-disks. One further disk position, y_2 , frequently arises in quenches; it is defined by the pentagonal arrangement of disks shown in Fig. 1(b).

The jammed states that we focus on in this paper (see Fig. 3) consist of tilted equilateral triangles of disks, separated by at least one pair of 1-disks. Refer to Fig. 2 which shows six disks (a,b,c,d,e,f) and their contacts with each other and the sides of the channel: (a) and (b) are nearest-neighbors lexically, and (a) and (c) next-nearest neighbors lexically (but (c) is physically closer to (a) than (b)). The triangles have varying orientations that are obtained via the following algorithm:

1. Disk (a) touches the wall, $y_a = \pm y_1$. An equilateral triangle of disks (b,c,d) has its first disk, (b), touching the opposite wall, $y_b = \mp y_1$, and its second disk, (c) (the apex of the equilateral triangle), touching disk (a). Given the values of (x_a, y_a) and (x_b, y_b) , the positions of disks (c) and (d) can be obtained exactly, e.g. by solving the four equations specifying the contacts (ac), (bc), (bd), and (cd).
2. Two more disks, (e) and (f), are placed at $\pm y_1$, touching their next-nearest neighbors, (c) and (d), respectively.
3. Steps 1 and 2 are repeated with disks (e) and (f) replacing (a) and (b), respectively.

At step (2) one could, instead of placing one pair of disks, choose to put in two pairs, as shown in Fig. 3(b): the stability of the jammed state is unaffected. States with a nonzero complexity can be obtained by placing the additional pairs of disks at random in the configuration generated by the deterministic algorithm 1–3.

The algorithm 1–3 generates configurations like those shown in Fig. 3(a) and (b). The y coordinates of the colored disks approach a limiting value, y_{teal} , which in our diagrams is represented by the color teal (intermediate between green and blue). The limiting state is crystalline; it is depicted in Fig. 4.

The jammed states in Fig. 3(a) and (b) do not satisfy periodic boundary conditions. Periodic states can be constructed as shown in Fig. 3(c), (e) and (f): two regions containing tilted equilateral triangles of disks are sandwiched between disks at positions 1 and 4, which form a region of buckled crystal. These sandwich states are characterized by an inversion of the tilted equilateral triangles near their midpoint.

III. MARGINAL STABILITY

We next discuss the stability of the sandwich states. They are manifestly *locally* jammed [42], as this only requires each disk to have three contacts, not all of which lie on the same half of the disk’s perimeter. We have checked these states for stability against a collective displacement of any number of

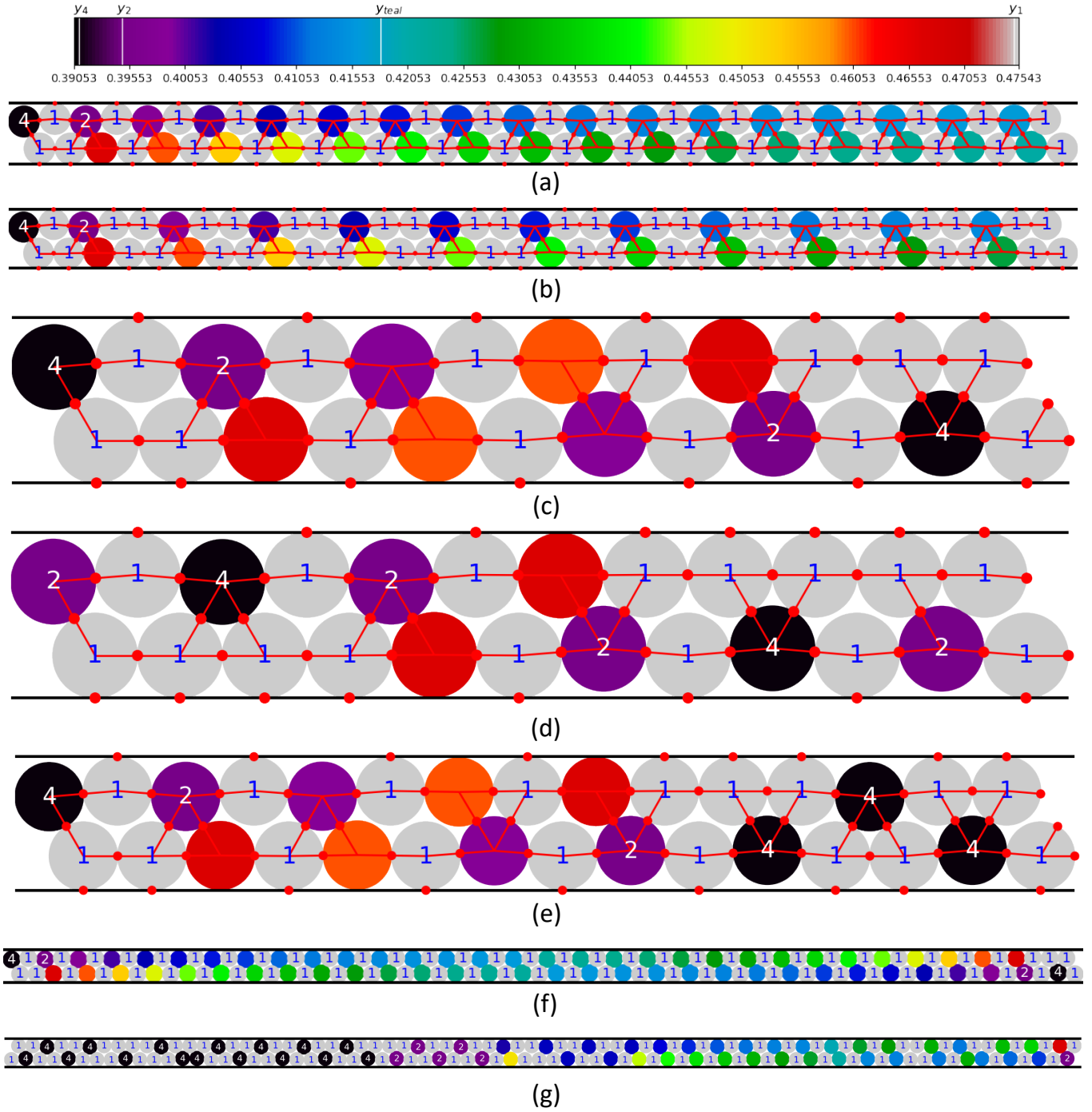


FIG. 3. Top: Color code for the y -coordinates of disks. (a) Colored disk pairs progressively approach the y -coordinates $\pm y_{\text{teal}} = \pm 0.41808$ associated with the color teal. (b) A jammed state where two pairs of disks have been inserted in positions y_1 . (c) A periodic “sandwich” state for $N = 24$. It has packing fraction $\phi = 0.80686$. This state is only locally jammed: on compression it evolves to the state (d), whose packing fraction is $\phi = 0.80688$. (e) A system of $N = 30 = (24 + 6)$ disks containing *two* unit cells of buckled crystal, which produces a state with more contacts. It is stable and has packing fraction $\phi = 0.80697$. (f) A stable sandwich state with $N = 128$. (g) A jammed state for $N = 150$ obtained after a Lubachevsky-Stillinger [41] quench from an initial state of packing fraction $\phi = 0.70$ to a final packing fraction $\phi = 0.807169$.

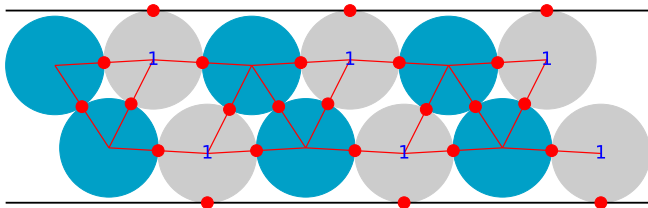


FIG. 4. Three unit cells of the limiting state that is approached in Fig. 3(a). The packing fraction $\phi \simeq 0.8068$. Note that in Fig. 3(a) there is always a gap between each pair of disks corresponding to disks (d) and (e) in Fig. 2; this gap is zero for the limiting state.

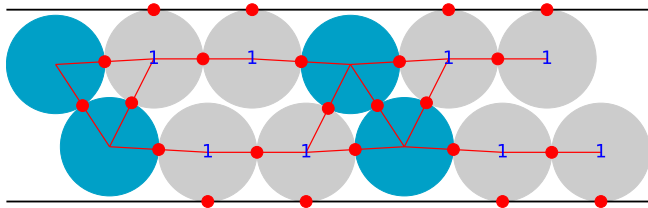


FIG. 5. Two unit cells of the limiting state that contains the maximum number of 1–1 insertions. It has packing fraction $\phi \simeq 0.8064$.

disks by using an extension of the linear programming algorithm discussed in Ref. [42]; details can be found in the Appendix. The algorithm not only checks for stability but also finds a stable state that the system can reach when it is not stable, as illustrated in Fig. 3(d) for the case $N = 24$. (Sandwich states with just one unit cell of buckled crystal within them have values of N which are multiples of 8.) We find that the sandwich states containing one unit cell of buckled crystal are stable for $N = 8$ and $N = 16$ and for all $N \geq 96$. However, for $N = 24, 32, \dots, 88$, the sandwich states can be made stable by the addition of a second unit cell of buckled crystal; an example is shown in Fig. 3(e) for the case $N = 24 + 6 = 30$.

The sandwich states can be regarded as marginally stable for large N . A truly marginal state is one in which the number of contacts of the disks is equal to the number of their degrees of freedom N_f . The latter is $2N - 1$ (not counting the uniform translation of the entire system along the x -axis); the number of contacts in periodic sandwich states with one unit cell of buckled crystal as shown in Fig. 3(c) is $N_c = 2N + 2$, so $N_c - N_f = 3$; i.e., there are just three more constraints than required for strict marginality. Thus, for large N (≥ 96), the sandwich states approach the condition of marginal stability, in the sense that the ratio $(N_c - N_f)/N$ can be made arbitrarily small by choosing a sufficiently large value for N .

IV. DETERMINATION OF THE EXPONENT γ

The marginally stable configurations have gaps that become vanishingly small for $N \rightarrow \infty$. They are the gaps between disks of types (d) and (e) in Fig. 2; see also Fig. 3(a). From the geometry of the state, the sizes h_i and h_{i+1} of consecutive gaps can be related algebraically. For large values of i , the

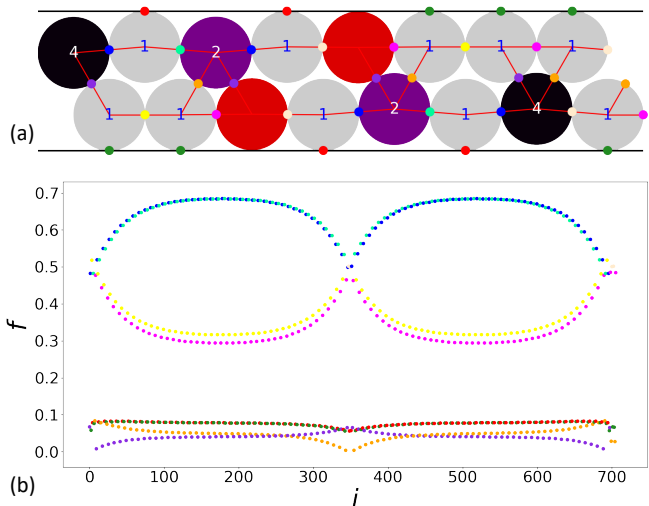


FIG. 6. (a) Color coding of contacts. (b) The force f at the i th contact in a sandwich state with $N = 352$ and $N_c = 706$, color coded as in (a). The smallest force is associated with the orange contacts at the center of the system, where the orientation of the equilateral triangles switches.

relation simplifies to

$$h_{i+1} = h_i/b, \quad (1)$$

where the constant $b \simeq 1.219$ for $h = 0.95\sigma$. This implies that for an infinite sequence the distribution of gaps would be of the form

$$g(h) = \frac{1}{h \ln b}, \quad (2)$$

as $h \rightarrow 0$; thus, the exponent for gap sizes is $\gamma = 1$. A distribution varying as $1/h$ at small h is not normalizable, but this is not a problem in practice because, for any finite value of N , there is a smallest gap whose size is of order $\exp(-cN)$, where $c > 0$. The result $\gamma = 1$ should be contrasted with $\gamma = 0.41269\dots$ for jammed states of spheres in the limit $d \rightarrow \infty$; the latter value of γ is also consistent with simulation results for all $d \geq 3$ [4].

Extra 1–1 disk insertions do not change the form of $g(h)$. Neither do they change the value of $N_c - N_f$; it remains at 3. Because any of the 1–1 pairs can be replaced by two 1–1 pairs, the total number of possible insertions is $2^{N/4-3}$, where N is the number of disks before the insertions are made. When N is large, the resulting states have packing fractions in the range $0.8064 < \phi < 0.8068$; the jammed states at the upper and lower limits of the density range are shown in Figs 4 and 5, respectively. Within this range of densities, the sandwich states are marginal and have a nonzero complexity.

States of the type discussed above consist of short lengths of buckled crystal alternating with noncrystalline regions of fixed length. Our construction can clearly be generalized to create aperiodic structures in which the lengths of the buckled-crystal and noncrystalline regions vary. We note that the distribution of small gaps, $g(h)$, will in general be related to the distribution of lengths of the noncrystalline regions, because

the size of the smallest gap in one of these regions depends (exponentially) on its length. It may also be noted that each additional region of buckled crystal increases the excess number of contacts, $N_c - N_f$, and so takes the system further from marginality.

Another much studied quantity for marginal jammed states is the exponent associated with the distribution of small contact forces f , $P(f) \sim f^\theta$. We used the algorithms in Ref. [43] to determine the forces in the contacts when a unit force is applied along the x axis. The smallest force, which occurs near the center of the sandwich state (see Fig. 6 for the case $N = 352$), seems to approach a nonzero value (≈ 0.005) as $N \rightarrow \infty$. The existence of a gap in $P(f)$ suggests that $\theta = \infty$. Notice that the inequality [44] $\gamma \geq 1/(2 + \theta)$ is satisfied by these values, as is the inequality $\gamma \geq (1 - \theta)/2$.

V. DISCUSSION

The sandwich state of Fig. 3(f) is a curious state of matter. In the limit of large N it approaches the crystalline state of Fig. 4. However, it never quite reaches that state: the equilateral triangles of disks all have slightly different orientations and the small gaps persist. If one were to compute the structure factor [45] of the state it would have for $N \rightarrow \infty$ the delta function peaks of the crystal in Fig. 4. It could thus be regarded as an asymptotic crystal. But if one regards it as a crystal, its unit cell is the length of the system. We suspect that similar states might already have been found in other systems with restricted geometries; for example, the packing of spheres within a long cylinder, as considered in Ref. [46], where certain jammed states, constructed so as to satisfy periodic boundary conditions, were found to have a unit cell that was as large as the system.

The study of Ikeda [36] of the jammed states of disks in a narrow channel in the presence of polydispersity produced a value of $\gamma = 0$, in contrast to our value in the absence of polydispersity, $\gamma = 1$. It is commonly assumed [40] that introducing polydispersity is ‘‘harmless’’; it merely serves to allow a speed up of simulations or to prevent crystallization. Our work shows that sometimes it completely changes the physics of the problem.

ACKNOWLEDGMENTS

We should like to thank P. Charbonneau, and E. Corwin for discussions. We would especially like to thank Harukuni Ikeda for many exchanges.

Appendix: The length-compression algorithm

This Appendix describes how we used a linear programming method to determine the stability of jammed states of

hard disks in a channel. Although the results are specific to our system, the methods are general and have been derived and discussed in detail by A. Donev and coworkers [42]. Our

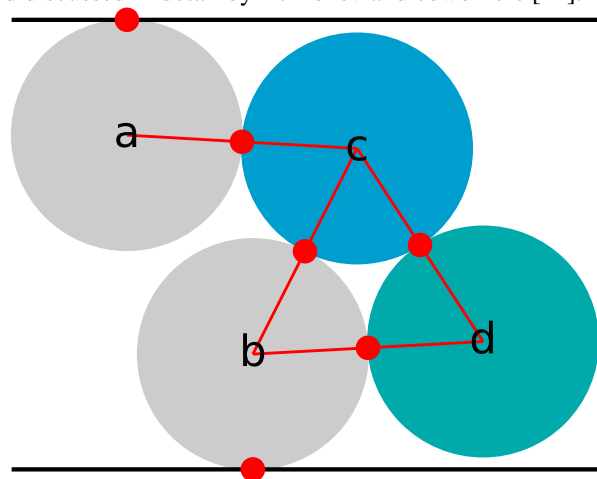


FIG. 7. A configuration of four disks, used in the example of a rigidity matrix given in Eq. (A.1). In addition to the actual contacts shown by red dots, the rigidity matrix includes potential contacts, such as those between disks (a) and (b), and between disks (c) and (d) and the walls.

discussion of the methods is therefore brief, and the reader is referred to Ref. [42] for a careful description.

If a jammed configuration of hard disks is unstable, that is, if it allows a collective motion of an arbitrary number of disks, then it can be compressed until the system is truly jammed. In our work we consider periodic configurations of N disks in a channel and minimize their length, subject to the constraints of no overlap of disks with each other or the channel walls. The length of the configuration, $L = x_{N+1} - x_1$, is a linear function of the $2N$ -dimensional vector of disk coordinates, \mathbf{R} . Thus, it is natural to consider a linear programming problem in which the function $L[\mathbf{R}]$ is minimized, subject to the following linearized constraints

$$\begin{aligned} \mathbf{A}^T \Delta \mathbf{R} &\geq -\mathbf{h}, \\ \Delta x_{N+1} &\leq 0, \\ \Delta x_1 &= 0, \\ \Delta \mathbf{r}_{N+1} &= \Delta \mathbf{r}_1, \\ \Delta \mathbf{r}_{N+2} &= \Delta \mathbf{r}_2, \end{aligned}$$

where $\Delta \mathbf{r}_n = (\Delta x_n, \Delta y_n)^T$, $\Delta \mathbf{R} = (\Delta \mathbf{r}_1, \Delta \mathbf{r}_2, \dots, \Delta \mathbf{r}_N)^T$ is a set of potential unjamming displacements, and \mathbf{A} is the *rigidity matrix* containing all potential contacts (i.e., pairwise contacts with all nearest and next-nearest neighbours). The components of the vector \mathbf{h} are the sizes of the gaps at each of the potential contacts; the gap sizes are nonnegative. The matrix \mathbf{A} has two rows for each disk and N_C columns that represent the N_C possible contacts. For the example shown in Fig. 7, \mathbf{A} is given by

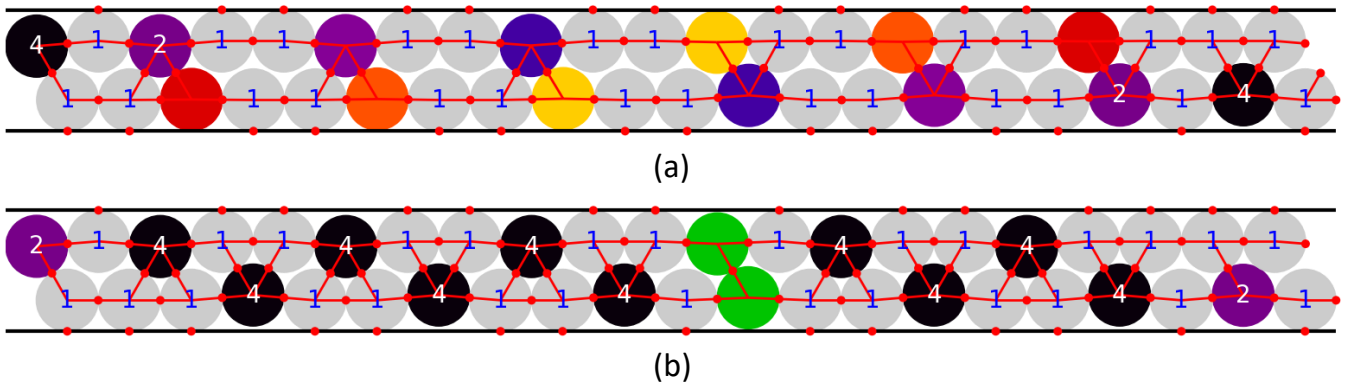


FIG. 8. Before, (a), and after, (b), the compression of an unstable configuration of $N = 42$ disks that contains the maximum possible number of 1–1 insertions in a sandwich state of 32 disks. The packing fraction of state (a) is $\phi = 0.80652$, which increases to 0.80721 on compression to the state (b).

$$\mathbf{A} = \begin{matrix} & a, w & a, b & a, c & b, w & b, c & b, d & c, w & c, d & d, w \\ \begin{matrix} a \\ b \\ c \\ d \end{matrix} & \begin{pmatrix} \mathbf{u}_{a,w} & \mathbf{u}_{a,b} & \mathbf{u}_{a,c} & 0 & 0 & 0 & 0 & 0 & 0 \\ 0 & -\mathbf{u}_{a,b} & 0 & \mathbf{u}_{b,w} & \mathbf{u}_{b,c} & \mathbf{u}_{b,d} & 0 & 0 & 0 \\ 0 & 0 & -\mathbf{u}_{a,c} & 0 & -\mathbf{u}_{b,c} & 0 & \mathbf{u}_{c,w} & \mathbf{u}_{c,d} & 0 \\ 0 & 0 & 0 & 0 & 0 & -\mathbf{u}_{b,d} & 0 & -\mathbf{u}_{c,d} & \mathbf{u}_{d,w} \end{pmatrix} \end{matrix}, \quad (\text{A.1})$$

where $\mathbf{u}_{m,n}$ denotes the unit vector directed from the center of disk n to the center of disk m ,

$$\mathbf{u}_{m,n} = \frac{\mathbf{r}_m - \mathbf{r}_n}{\|\mathbf{r}_m - \mathbf{r}_n\|},$$

and $\mathbf{u}_{m,w} = \pm \hat{y}$ is a unit vector directed into the channel from the wall that is nearer to disk m . To implement the periodic boundary condition, two extra disks $N + 1$ and $N + 2$, which are equivalent to disks 1 and 2, are added to the end of the channel; this avoids having the matrix \mathbf{A} depend on L , which would make the problem nonlinear. The bottom right section of \mathbf{A} containing these disks is then

$$\begin{matrix} \vdots \\ N-1 \\ N \\ N+1 \\ N+2 \end{matrix} \begin{pmatrix} \cdots & N-1, w & N-1, N & N-1, N+1 & N, w & N, N+1 & N, N+2 \\ \ddots & & & & & & \\ \mathbf{u}_{N-1,w} & \mathbf{u}_{N-1,N} & \mathbf{u}_{N-1,N+1} & 0 & 0 & 0 \\ 0 & -\mathbf{u}_{N-1,N} & 0 & \mathbf{u}_{N,w} & \mathbf{u}_{N,N+1} & \mathbf{u}_{N,N+2} \\ 0 & 0 & -\mathbf{u}_{N-1,N+1} & 0 & -\mathbf{u}_{N,N+1} & 0 \\ 0 & 0 & 0 & 0 & 0 & -\mathbf{u}_{N,N+2} \end{pmatrix},$$

and the displacements of disks $N + 1$ and $N + 2$ are defined by the last two linear constraints, $\Delta \mathbf{r}_{N+1} = \Delta \mathbf{r}_1$ and $\Delta \mathbf{r}_{N+2} = \Delta \mathbf{r}_2$.

The solution of the linear programming problem described above provides a set of displacements that reduces the length of the system. It is easily shown [42] that any set of displacements that satisfy the linearized nonoverlap constraints will also satisfy the exact (nonlinear) constraints. Thus, to obtain the densest packing we apply these displacements, recalculate \mathbf{A} , and then repeat the process until no further displacement of the disks will reduce the length. For our minimum-length configurations with strict zigzag order, we find that there is no room for disks to “rattle”: the system has reached a jammed state. Our stopping criterion was chosen as $\Delta L < 10^{-8} \sigma$, as

this is a typical observed order of magnitude for changes when the algorithm is applied to a known stable configuration, such as the buckled crystal. When a state is stable the final state is, of course, the same as the initial state, to within the numerical precision of the calculation.

The sandwich states, with and without the insertion of extra pairs of disks at positions $\pm y_1$, were compressed using the iterative algorithm described above. In the main text we have shown the result of compressing the $N = 24$ sandwich state containing no extra disks at $\pm y_1$; see Fig. 3(c,d). Another example for which the sandwich state is found to be unstable is shown in Fig. 8 for the case $N = 32 + 10$, which contains the maximum number of insertions of disks at $\pm y_1$ into a sandwich state of 32 disks. The configuration is unstable when

only one unit cell of buckled crystal is included (as shown

in Fig. 8(a)), but becomes stable if two unit cells of buckled crystal are present.

-
- [1] Matthieu Wyart, “Marginal Stability Constrains Force and Pair Distributions at Random Close Packing,” *Phys. Rev. Lett.* **109**, 125502 (2012).
- [2] Markus Müller and Matthieu Wyart, “Marginal Stability in Structural, Spin, and Electron Glasses,” *Annual Review of Condensed Matter Physics* **6**, 177–200 (2015).
- [3] Ada Altieri, “The Jamming Transition,” in *Jamming and Glass Transitions: In Mean-Field Theories and Beyond* (Springer International Publishing, Cham, 2019) pp. 45–64.
- [4] Patrick Charbonneau, Eric I. Corwin, Giorgio Parisi, and Francesco Zamponi, “Universal Microstructure and Mechanical Stability of Jammed Packings,” *Phys. Rev. Lett.* **109**, 205501 (2012).
- [5] Silvio Franz, Giorgio Parisi, Maksim Sevelev, Pierfrancesco Urbani, and Francesco Zamponi, “Universality of the SAT-UNSAT (jamming) threshold in non-convex continuous constraint satisfaction problems,” *SciPost Phys.* **2**, 019 (2017).
- [6] Jorge Kurchan, Giorgio Parisi, Pierfrancesco Urbani, and Francesco Zamponi, “Exact Theory of Dense Amorphous Hard Spheres in High Dimension. II. The High Density Regime and the Gardner Transition,” *The Journal of Physical Chemistry B* **117**, 12979–12994 (2013).
- [7] Patrick Charbonneau, Jorge Kurchan, Giorgio Parisi, Pierfrancesco Urbani, and Francesco Zamponi, “Exact theory of dense amorphous hard spheres in high dimension. III. The full replica symmetry breaking solution,” *Journal of Statistical Mechanics: Theory and Experiment* **2014**, P10009 (2014).
- [8] Patrick Charbonneau, Jorge Kurchan, Giorgio Parisi, Pierfrancesco Urbani, and Francesco Zamponi, “Glass and Jamming Transitions: From Exact Results to Finite-Dimensional Descriptions,” *Annual Review of Condensed Matter Physics* **8**, 265–288 (2017).
- [9] G. Parisi, “Infinite number of order parameters for spin-glasses,” *Phys. Rev. Lett.* **43**, 1754 (1979).
- [10] Giorgio Parisi, Yoav G. Pollack, Itamar Procaccia, Corrado Rainone, and Murari Singh, “Robustness of mean field theory for hard sphere models,” *Phys. Rev. E* **97**, 063003 (2018).
- [11] Peter Olsson, “Dimensionality and Viscosity Exponent in Shear-driven Jamming,” *Phys. Rev. Lett.* **122**, 108003 (2019).
- [12] Matthieu Wyart, Leonardo E. Silbert, Sidney R. Nagel, and Thomas A. Witten, “Effects of compression on the vibrational modes of marginally jammed solids,” *Phys. Rev. E* **72**, 051306 (2005).
- [13] Wyart, M., “On the rigidity of amorphous solids,” *Ann. Phys. Fr.* **30**, 1–96 (2005).
- [14] Andrea J. Liu and Sidney R. Nagel, “The Jamming Transition and the Marginally Jammed Solid,” *Annual Review of Condensed Matter Physics* **1**, 347–369 (2010).
- [15] Carl P. Goodrich, Andrea J. Liu, and Sidney R. Nagel, “Finite-Size Scaling at the Jamming Transition,” *Phys. Rev. Lett.* **109**, 095704 (2012).
- [16] Daniel Hexner, Andrea J. Liu, and Sidney R. Nagel, “Two diverging length scales in the structure of jammed packings,” *Phys. Rev. Lett.* **121**, 115501 (2018).
- [17] Daniel Hexner, Pierfrancesco Urbani, and Francesco Zamponi, “Can a large packing be assembled from smaller ones?” *Phys. Rev. Lett.* **123**, 068003 (2019).
- [18] Carl P. Goodrich, Simon Dagois-Bohy, Brian P. Tighe, Martin van Hecke, Andrea J. Liu, and Sidney R. Nagel, “Jamming in finite systems: Stability, anisotropy, fluctuations, and scaling,” *Phys. Rev. E* **90**, 022138 (2014).
- [19] Merlijn S. van Deen, Johannes Simon, Zorana Zeravcic, Simon Dagois-Bohy, Brian P. Tighe, and Martin van Hecke, “Contact changes near jamming,” *Phys. Rev. E* **90**, 020202 (2014).
- [20] Daniel Vågberg, Peter Olsson, and S. Teitel, “Critical scaling of Bagnold rheology at the jamming transition of frictionless two-dimensional disks,” *Phys. Rev. E* **93**, 052902 (2016).
- [21] J. F. Robinson, M. J. Godfrey, and M. A. Moore, “Glasslike behavior of a hard-disk fluid confined to a narrow channel,” *Phys. Rev. E* **93**, 032101 (2016).
- [22] M. J. Godfrey and M. A. Moore, “Understanding the ideal glass transition: Lessons from an equilibrium study of hard disks in a channel,” *Phys. Rev. E* **91**, 022120 (2015).
- [23] M. J. Godfrey and M. A. Moore, “Static and dynamical properties of a hard-disk fluid confined to a narrow channel,” *Phys. Rev. E* **89**, 032111 (2014).
- [24] R. K. Bowles and I. Saika-Voivod, “Landscapes, dynamic heterogeneity, and kinetic facilitation in a simple off-lattice model,” *Phys. Rev. E* **73**, 011503 (2006).
- [25] Mahdi Zaeifi Yamchi, S. S. Ashwin, and Richard K. Bowles, “Fragile-strong fluid crossover and universal relaxation times in a confined hard-disk fluid,” *Phys. Rev. Lett.* **109**, 225701 (2012).
- [26] S. S. Ashwin, Mahdi Zaeifi Yamchi, and Richard K. Bowles, “Inherent structure landscape connection between liquids, granular materials, and the jamming phase diagram,” *Phys. Rev. Lett.* **110**, 145701 (2013).
- [27] Mahdi Zaeifi Yamchi, S. S. Ashwin, and Richard K. Bowles, “Inherent structures, fragility, and jamming: Insights from quasi-one-dimensional hard disks,” *Phys. Rev. E* **91**, 022301 (2015).
- [28] D. A. Kofke and A. J. Post, “Hard particles in narrow pores. Transfer matrix solution and the periodic narrow box,” *J. Chem. Phys.* **98**, 4853 (1993).
- [29] S. Varga, G. Balló, and P. Gurin, “Structural properties of hard disks in a narrow tube,” *Journal of Statistical Mechanics: Theory and Experiment* **2011**, P11006 (2011).
- [30] P. Gurin and S. Varga, “Pair correlation functions of two- and three-dimensional hard-core fluids confined into narrow pores: Exact results from transfer matrix method,” *J. Chem. Phys.* **139**, 244708 (2013).
- [31] Yi Hu, Lin Fu, and Patrick Charbonneau, “Correlation lengths in quasi-one-dimensional systems via transfer matrices,” *Molecular Physics* **116**, 3345 (2018).
- [32] C. L. Hicks, M. J. Wheatley, M. J. Godfrey, and M. A. Moore, “Gardner transition in physical dimensions,” *Phys. Rev. Lett.* **120**, 225501 (2018).
- [33] A. Huerta, T. Bryk, V. M. Pergamenschchik, and A. Trokhymchuk, “Kosterlitz-thouless-type caging-uncaging transition in a quasi-one-dimensional hard disk system,” *Phys. Rev. Research* **2**, 033351 (2020).
- [34] M. J. Godfrey and M. A. Moore, “Absence of Hyperuniformity in Amorphous Hard-Sphere Packings of Nonvanishing Complexity,” *Phys. Rev. Lett.* **121**, 075503 (2018).

- [35] S. S. Ashwin and Richard K. Bowles, “Complete jamming landscape of confined hard discs,” *Phys. Rev. Lett.* **102**, 235701 (2009).
- [36] Harukuni Ikeda, “Jamming Below Upper Critical Dimension,” *Phys. Rev. Lett.* **125**, 038001 (2020).
- [37] Ludovic Berthier, Patrick Charbonneau, and Joyjit Kundu, “Bypassing sluggishness: SWAP algorithm and glassiness in high dimensions,” *Phys. Rev. E* **99**, 031301 (2019).
- [38] Romain Mari, Florent Krzakala, and Jorge Kurchan, “Jamming versus glass transitions,” *Phys. Rev. Lett.* **103**, 025701 (2009).
- [39] Patrick Charbonneau, Eric I. Corwin, Lin Fu, Georgios Tsekenis, and Michael van der Naald, “Glassy, Gardner-like phenomenology in minimally polydisperse crystalline systems,” *Phys. Rev. E* **99**, 020901 (2019).
- [40] Harukuni Ikeda, “Jamming and replica symmetry breaking of weakly disordered crystals,” *Phys. Rev. Research* **2**, 033220 (2020).
- [41] Boris D. Lubachevsky and Frank H. Stillinger, “Geometric properties of random disk packings,” *Journal of Statistical Physics* **60**, 561 (1990).
- [42] Aleksander Donev, Salvatore Torquato, Frank H. Stillinger, and Robert Connelly, “A linear programming algorithm to test for jamming in hard-sphere packings,” *Journal of Computational Physics* **197**, 139 – 166 (2004).
- [43] Patrick Charbonneau, Eric I. Corwin, Giorgio Parisi, and Francesco Zamponi, “Jamming Criticality Revealed by Removing Localized Buckling Excitations,” *Phys. Rev. Lett.* **114**, 125504 (2015).
- [44] Edan Lerner, Gustavo Düring, and Matthieu Wyart, “Low-energy non-linear excitations in sphere packings,” *Soft Matter* **9**, 8252 (2013).
- [45] A Hof, “On diffraction by aperiodic structures,” *Communications in Mathematical Physics* **169**, 25 (1995).
- [46] Lin Fu, William Steinhardt, Hao Zhao, Joshua E. S. Socolar, and Patrick Charbonneau, “Hard sphere packings within cylinders,” *Soft Matter* **12**, 2505 (2016).